

## Accepted Manuscript

### 1-Benzyl-4-Phenyl-1*H*-1,2,3-Triazoles Improve the Transcriptional Functions of Estrogen-Related Receptor $\gamma$ and Promote the Browning of White Adipose

Shilin Xu, Liufeng Mao, Ping Ding, Xiaoxi Zhuang, Yang Zhou, Lei Yu, Yingxue Liu, Tao Nie, Tingting Xu, Yong Xu, Jinsong Liu, Jeff Smail, Xiaomei Ren, Donghai Wu, Ke Ding

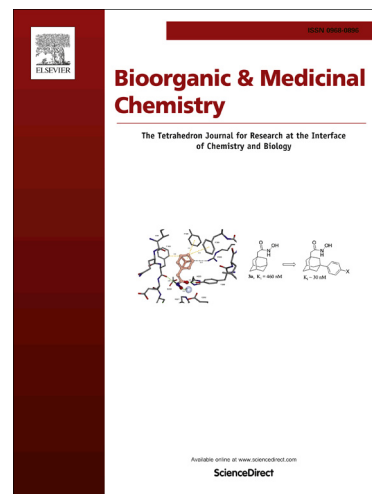
PII: S0968-0896(15)00278-3  
DOI: <http://dx.doi.org/10.1016/j.bmc.2015.03.082>  
Reference: BMC 12208

To appear in: *Bioorganic & Medicinal Chemistry*

Received Date: 22 February 2015  
Revised Date: 30 March 2015  
Accepted Date: 31 March 2015

Please cite this article as: Xu, S., Mao, L., Ding, P., Zhuang, X., Zhou, Y., Yu, L., Liu, Y., Nie, T., Xu, T., Xu, Y., Liu, J., Smail, J., Ren, X., Wu, D., Ding, K., 1-Benzyl-4-Phenyl-1*H*-1,2,3-Triazoles Improve the Transcriptional Functions of Estrogen-Related Receptor  $\gamma$  and Promote the Browning of White Adipose, *Bioorganic & Medicinal Chemistry* (2015), doi: <http://dx.doi.org/10.1016/j.bmc.2015.03.082>

This is a PDF file of an unedited manuscript that has been accepted for publication. As a service to our customers we are providing this early version of the manuscript. The manuscript will undergo copyediting, typesetting, and review of the resulting proof before it is published in its final form. Please note that during the production process errors may be discovered which could affect the content, and all legal disclaimers that apply to the journal pertain.



# 1-Benzyl-4-Phenyl-1*H*-1,2,3-Triazoles Improve the Transcriptional Functions of Estrogen-Related Receptor $\gamma$ and Promote the Browning of White Adipose

*Shilin Xu,<sup>†,#</sup> Liufeng Mao,<sup>†,#</sup> Ping Ding,<sup>†,§,#</sup> Xiaoxi Zhuang,<sup>†</sup> Yang Zhou,<sup>†</sup> Lei Yu,<sup>†</sup> Yingxue Liu,<sup>†</sup>  
Tao Nie,<sup>†</sup> Tingting Xu,<sup>†</sup> Yong Xu,<sup>†</sup> Jinsong Liu,<sup>†</sup> Jeff Smaill,<sup>‡,ϕ</sup> Xiaomei Ren,<sup>\*†</sup> Donghai Wu,<sup>\*†</sup>  
and Ke Ding<sup>\*†</sup>*

<sup>†</sup> State Key Laboratory of Respiratory Diseases, Guangzhou Institutes of Biomedicine and Health,  
Chinese Academy of Sciences, No. 190 Kaiyuan Avenue, Guangzhou 510530, China

<sup>§</sup> School of Life Science, Anhui University, Hefei 230601, Anhui, China

<sup>‡</sup>Auckland Cancer Society Research Centre, University of Auckland, #92019 Private Bag ,

Auckland 1142, New Zealand

<sup>ϕ</sup>Maurice Wilkins Centre for Molecular Biodiscovery, University of Auckland, #92019 Private

Bag, Auckland 1142, New Zealand

**KEYWORDS.** Estrogen-Related Receptor  $\gamma$ , adipose browning, drug design, triazole

**ABSTRACT.** The estrogen-related receptor  $\gamma$  (ERR $\gamma$ ) is a potential molecular target for the development of small molecules to stimulate the adipose browning process, which may represent a novel attractive strategy to treat obesity related disorders. The receptor possesses a very small ligand binding cavity and therefore identification of small molecule ERR $\gamma$  modulators is a considerable challenge. We have successfully designed and synthesized a series of 1-benzyl-4-phenyl-1*H*-1, 2, 3-triazoles and demonstrated that they improve the transcriptional functions of ERR $\gamma$ , potently elevating both the mRNA levels and the protein levels of ERR $\gamma$  downstream targets. One of the most promising compounds, 4-(1-(4-iso-propylbenzyl)-1*H*-1,2,3-triazol-4-yl)benzene-1,2-diol (**2e**) was further shown to directly bind with the ERR $\gamma$  ligand binding domain (ERR $\gamma$ -LBD) in an isothermal calorimetric (ITC) assay and to thermally stabilize ERR $\gamma$ -LBD protein by increasing its melting temperature ( $T_m$ ) as demonstrated by circular dichroism (CD) spectroscopy. Furthermore, **2e** potently stimulates the adipocyte browning process and induces mitochondrial biogenesis both *in vitro* and *in vivo*, suggesting the considerable therapeutic potential of this compound for the treatment of obesity and related disorders.

## INTRODUCTION

Two types of adipose tissues have been identified in mammals, i.e. white adipose tissue (WAT) and brown adipose tissue (BAT).<sup>1</sup> WAT is located predominantly in the subcutaneous and visceral organs where it stores excess energy in the form of triglycerides. Excessive accumulation of WAT is the primary cause of obesity and can eventually lead to type 2 diabetes, cardiovascular disease and other metabolic disorders.<sup>2</sup> BAT, on the other hand, stores lipids in a multilocular droplet morphology and possesses much higher mitochondrial content than WAT.

The key functions of BAT are to burn fat for body heat production (adaptive thermogenesis) and to promote weight loss by increasing energy expenditure.<sup>3</sup> Although controversy had been associated with the occurrence of BAT in adult humans, recent data derived from a positron-emission-tomography (PET) study convincingly demonstrated the existence of active BAT in adults.<sup>4</sup> Different reports have shown that exposure to cold temperatures or expression of several endogenous ligands (e.g. Irisin<sup>5</sup>, FGF21<sup>6</sup>) can induce the presence of brown-like adipocytes (also known as beige cells) in WAT tissue and cause the weight loss of animals.<sup>7</sup> The WAT → BAT transition has been termed biologically as adipose browning. Promoting the browning process in white adipose tissue and/or activation of the function of BAT by small molecules becomes a highly attractive strategy to treat obesity and its related complications.<sup>8</sup> Several molecules have been reported to stimulate the adipose browning process with different mechanisms of action (MOA).<sup>3b</sup> However, none of these molecules have been advanced into clinical investigation for the treatment of obesity. It is highly desirable to identify new molecules with different MOA to promote the browning of white adipose.

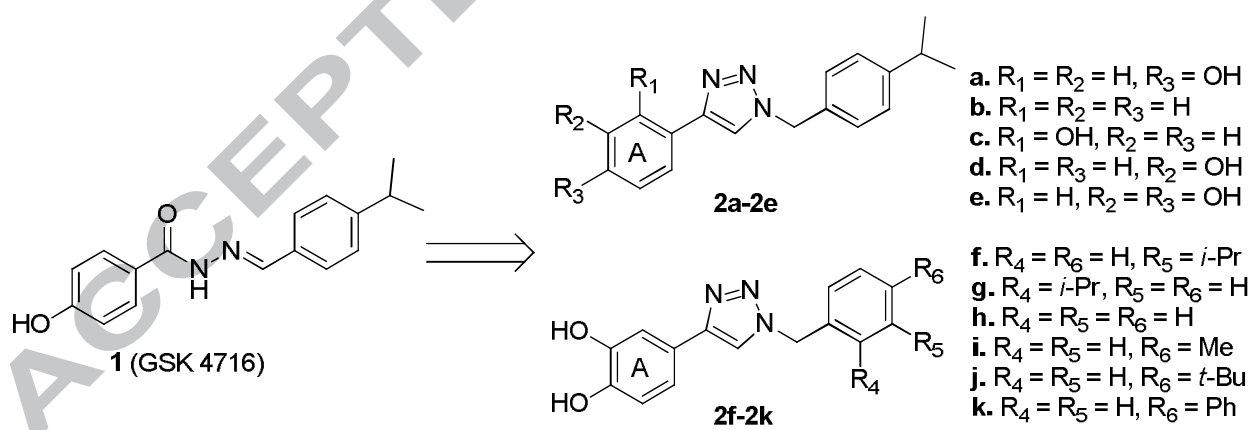


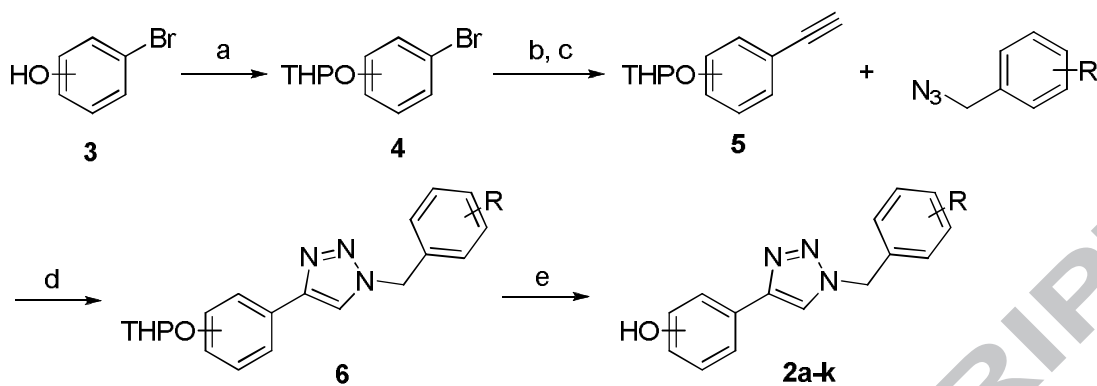
**Chart 1.** Design of 1-benzyl-4-phenyl-1*H*-1,2,3-triazole derivatives as new ERR $\gamma$  agonists by scaffolding hopping of reported compound **1** (GSK4716).

It was recently reported that transfection of estrogen-related receptor  $\gamma$  (ERR $\gamma$ ) could remarkably enhance the expression of uncoupling protein 1 (UCP1), a brown-fat specific gene, and improve fatty acid oxidation in differentiating white pre-adipocytes and/or BAT, suggesting ERR $\gamma$  could be a new promising target for development of small molecules to induce adipose browning.<sup>9</sup> ERR $\gamma$  belongs to an orphan nuclear receptor subfamily<sup>10</sup> and is expressed mainly in energy-dependent tissues including the brain, heart, kidney, skeletal muscle and BAT.<sup>11</sup> It has been demonstrated that ERR $\gamma$  possesses a small ligand binding pocket less than 280 Å<sup>3</sup> in volume, highlighting the challenge to identify small molecules regulating this receptor.<sup>12</sup> Only recently, GSK4716 (**1**, Chart **1**) and closely related derivatives were reported to selectively upregulate the transcriptional functions of ERR $\gamma$ .<sup>13</sup> However, to the best of our knowledge, there has been no report of using a small molecule ERR $\gamma$  modulator to induce adipose browning. Herein, we describe the design of new molecules improving the transcriptional functions of ERR $\gamma$ . Furthermore, one of the representative molecules, **2e**, potently stimulates the browning process of white adipose.

## CHEMISTRY

The rationally designed compounds were readily synthesized using the procedures shown in scheme **1**. Briefly, the hydroxyl substituted bromobenzene starting materials **3** were protected with 3,4-dihydro-2*H*-pyran (DHP) to give the compounds **4**. Pd-catalyzed Sonogashira coupling of these with trimethylsilylacetylene (TMSA) followed by treatment of K<sub>2</sub>CO<sub>3</sub> in methanol gave the acetylene derivatives **5**. These underwent a Cu-catalyzed “click” cycloaddition with the self-prepared benzyl azides to obtain the triazole intermediates **6**, which were further deprotected to provide the products **2a-2k**.

**Scheme 1.** Synthesis of compounds **2a-2k** <sup>a</sup>



<sup>a</sup> Reagents and conditions: (a) 3,4-Dihydro-2*H*-pyran, pyridinium *p*-toluenesulfonate, CH<sub>2</sub>Cl<sub>2</sub>, rt; (b) Trimethylsilylacetylene, PdCl<sub>2</sub>(PPh<sub>3</sub>)<sub>2</sub>, CuI, triethylamine, 80 °C; (c) K<sub>2</sub>CO<sub>3</sub>, MeOH, rt; (d) Sodium ascorbate, CuSO<sub>4</sub>, t-BuOH/H<sub>2</sub>O (1:1), rt; (e) Pyridinium *p*-toluenesulfonate, EtOH, 50 °C.

## RESULTS AND DISCUSSION

Structural feature analysis of the ERR $\gamma$ -compound **1** complex (PDB: 2GPP) clearly revealed a conformational rearrangement of ERR $\gamma$  induced by compound **1**, resulting in an accessible rear pocket originally shielded by a salt-bridge between Glu275 and Arg316. The phenolic hydroxyl and acyl hydrazone moieties in **1** participate in critical hydrogen bond networks with various residues of the protein, while the isopropyl group is held in a small hydrophobic cavity by Van der Waals interactions.<sup>12</sup> Based on the structural information of the compound **1**-ERR $\gamma$  complex, we successfully designed compound **2a** as a new potential ERR $\gamma$  modulator in which the 1,2,3-triazole moiety could be considered as a non-classical bioisostere of the acyl hydrazone moiety of compound **1**.<sup>14</sup> Modeling studies suggested that, similarly to **1**, compound **2a** could bind the conformationally rearranged ligand binding domain of ERR $\gamma$  (ERR $\gamma$ -LBD, Figure **1a**). However,

the hydroxyl substituent of **2a** is predicted to form a strong hydrogen bond with Glu247 of the protein, while the corresponding residue for compound **1** is Asp328.

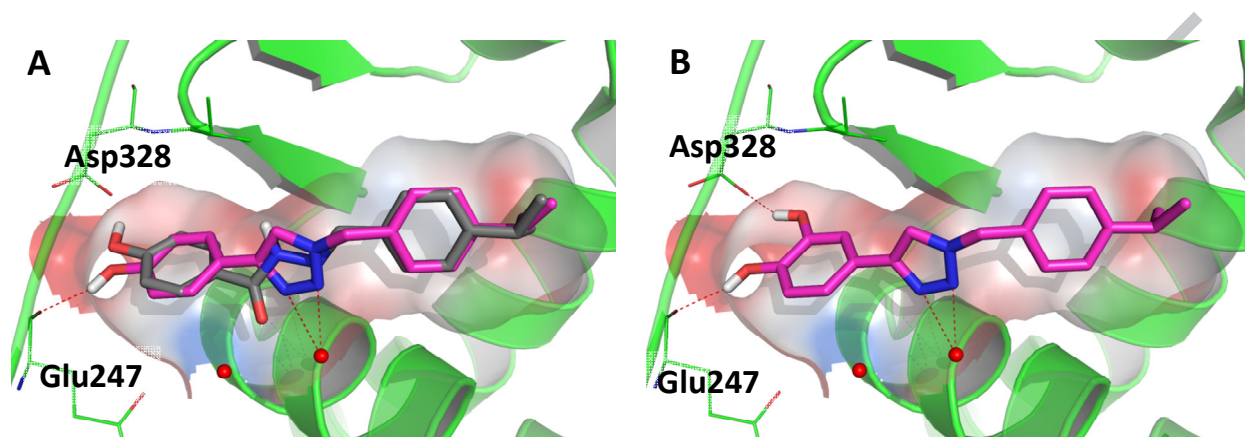


**Figure 1.** Predicted binding modes of compounds **2a** and **2e** with ERR $\gamma$ -LBD. a) Predicted binding mode of **2a** (magenta carbons) in the LBD of ERR $\gamma$  (PDB: 2GPP), and superposition of **2a** with compound **1** (dark gray carbons). b) Predicted binding mode of **2e** (magenta carbons) with ERR $\gamma$ -LBD. The ligands are showed in stick model, while the ERR $\gamma$  protein is shown in cartoon model. The key residues are shown in a line model, and the water molecules are depicted as red spheres.

Preliminary determination of the modulating effect of **2a** on ERR $\gamma$  was accomplished by a well-established mammalian two-hybrid reporter gene assay at 2.0  $\mu$ M using compound **1** as a positive control for parallel comparison (Figure 2).<sup>15</sup> Under the screening conditions, compound **1** potently improved the transcriptional function of ERR $\gamma$  by a factor of 1.85-fold which is comparable to the reported results.<sup>13a</sup> Compound **2a** displayed an almost identical effect on ERR $\gamma$  transcriptional activity. Further structure-activity relationship (SAR) investigation revealed that the 4-hydroxyl group in ring A of **2a** might be critical for its effect on ERR $\gamma$ . When the 4-hydroxyl group is removed (**2b**) or is moved to the 2- position as in **2c**, the resulting compounds

showed weaker regulatory effects on ERR $\gamma$ . Interestingly, the 3-hydroxyl derivative (**2d**) displayed slightly improved potency, potentially resulting from this substituent forming a favorable hydrogen bond with Asp328 of the protein. The 3,4-dihydroxyl compound **2e** significantly elevated the transcriptional function of ERR $\gamma$  by a factor of 5-fold at 2.0  $\mu$ M, and is obviously more potent than **2a** or **2d**. A preliminary computational investigation suggests **2e** may form two hydrogen bonds with Asp328 and Glu247, respectively, and thus achieve improved bioactivity (Figure **1b**). It is noteworthy that the catechol scaffold in **2e** has been identified in a number of FDA approved drugs including Dopamine and Northera, despite the general belief that it is a pharmaceutically unfavorable group. Further investigation demonstrated that the compound's effect on ERR $\gamma$  is dose-dependent (Supporting Information, Figure **S3**). The impact of the substituent in ring B was also investigated and it was clearly revealed that a *para*-isopropyl group is optimal; when the isopropyl group in **2e** is moved to the *m*- (**2f**) or the *o*-position (**2g**), the potency decreases considerably. Other compounds with smaller or larger substituents, such as H (**2h**), methyl (**2i**), *tert*-butyl (**2j**) and phenyl (**2k**), are also less potent. Thus, **2e** represents one of the most potent compounds for further biological investigation.

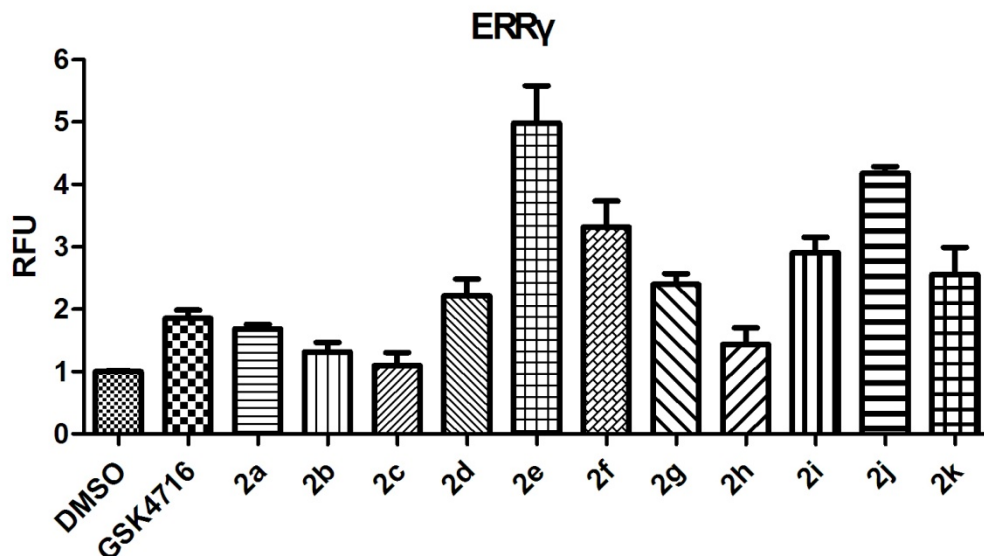


**Figure 2.** 1-Benzyl-4-phenyl-1*H*-1,2,3-triazole derivatives upregulate the transcriptional function of ERR $\gamma$  at 2.0  $\mu$ M in a mammalian two-hybrid reporter gene assay. Results are the mean ( $\pm$  SEM) of at least three independent experiments.

The effect of **2e** on the improvement of the transcriptional function of ERR $\gamma$  was further validated by investigating its impact on the expression of ERR $\gamma$  targeted genes, such as SHP (small heterodimer partner)<sup>16</sup>, ERR $\alpha$ <sup>17</sup>, ATP5b (ATP synthase 5b)<sup>11c, 18</sup> and MCAD (medium-chain acyl-coenzyme A dehydrogenase).<sup>18</sup> It was shown that **2e** dose-dependently elevated the mRNA levels of these genes in a quantitative real-time PCR assay, while the less potent compound **2c** failed to show much effect at 1.0  $\mu$ M. It was also noteworthy that the mRNA level of ERR $\gamma$  is also increased after exposure to compound **2e**.<sup>19</sup> Further investigation revealed that **2e** also significantly increased the levels of ATP5b and MCAD proteins in a western blot assay (Figure 3).

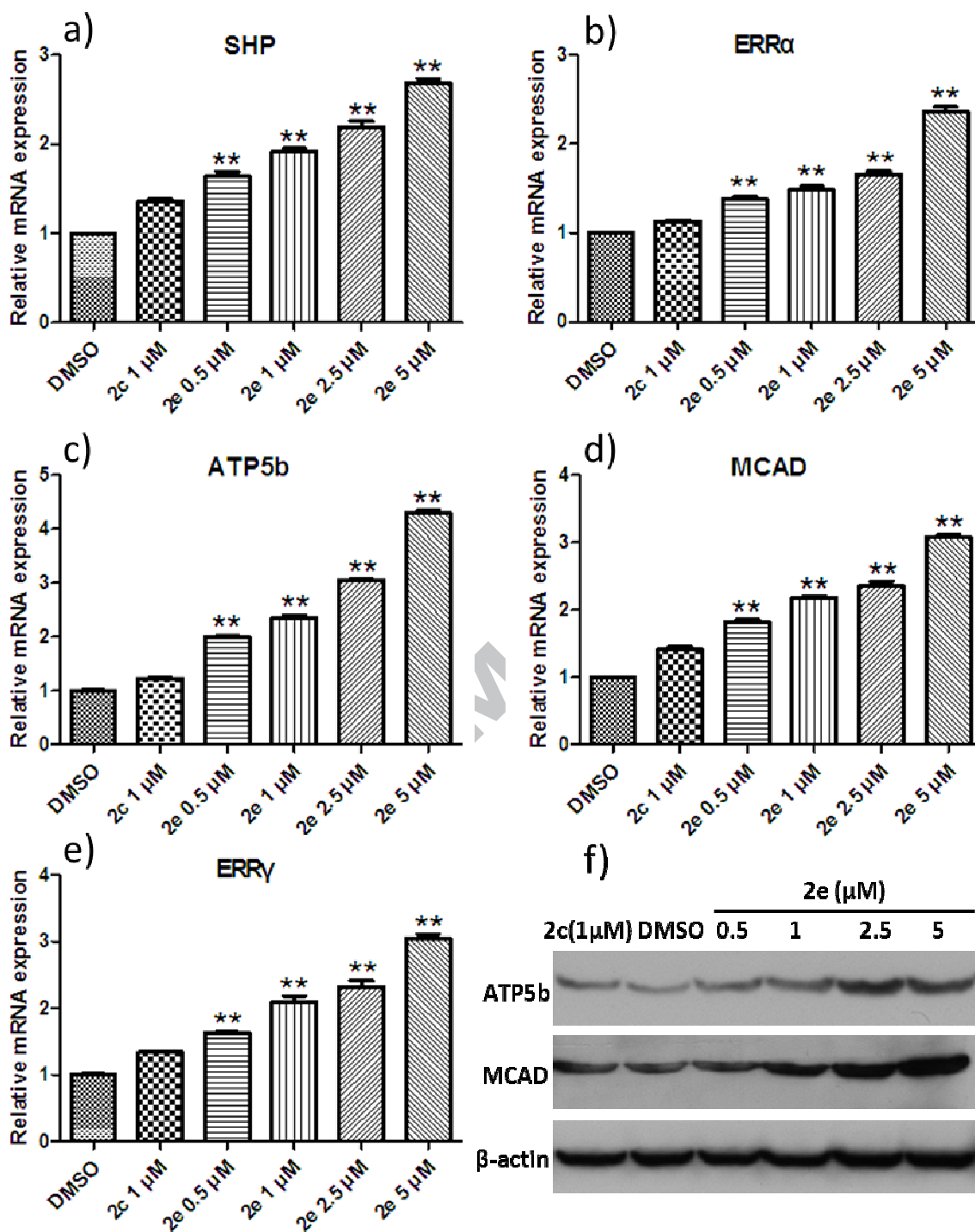


**Figure 3.** Compound **2e** upregulates the transcriptional functions of ERR $\gamma$ . a-e) **2e** elevated the mRNA levels of SHP, ERR $\alpha$ , ATP5b, MCAD and ERR $\gamma$  in a quantitative real-time PCR assay. f) **2e** increased the protein levels of ATP5b and MCAD determined by a western blot assay.

ATP5b and MCAD proteins were detected at a size of 52 and 43 kDa, respectively. Results are the mean ( $\pm$  SEM) or representative of three independent experiments (\*\*P < 0.01).

The direct binding of compound **2e** with ERR $\gamma$ -LBD was also examined in an isothermal calorimetric (ITC) assay. It was confirmed that **2e** indeed could bind to the protein with an experimental  $K_d$  value of 46.0  $\mu$ M at 20 °C (Figure 4), about 10-fold weaker than compound **1** ( $K_d$  = 5.0  $\mu$ M, data not shown) under the same assay conditions. Further investigation by circular dichroism (CD) assay showed a small increase in the melting temperature ( $T_m$ ) by 0.7 °C when compound **2e** was added (Supporting Information, Table S1). A comparable increase in the  $T_m$  for compound **1** was reported.<sup>12</sup> The discrepancy between the weak protein binding affinity and its relatively strong effect on improving transcriptional function suggests that compound **2e** may achieve ERR $\gamma$  modulating activity through a different mechanism than that of compound **1**.

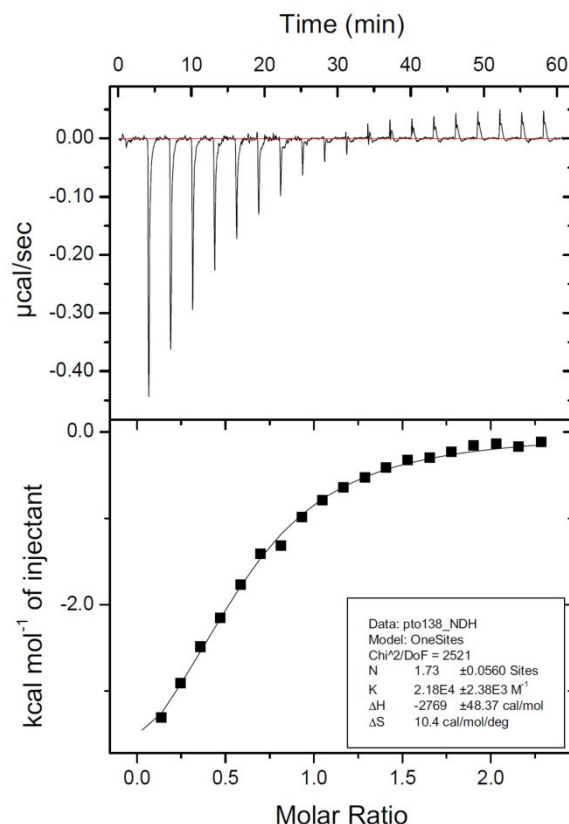


**Figure 4.** Isothermal calorimetric analysis of the binding interaction between ERR $\gamma$ -LBD and compound **2e**.

The ability of **2e** to drive adipose browning was also examined by studying its effect on the expression of UCP1 in white adipocytes derived from mouse embryonic fibroblasts (MEF). It was shown that **2e** dose-dependently induced the elevation of UCP1 both at the mRNA and protein level (Figure **5a** and **5b**). Further study revealed that **2e** also markedly increased the number of UCP1-positive adipocytes in an immunofluorescence staining assay (Figure **5c**). It is noteworthy that another brown-fat-selective gene, Prdm16<sup>20</sup>, was also significantly elevated in MEF-derived adipocytes after **2e** treatment (Supporting Information, Figure **S4**). Moreover, a similar browning effect of **2e** could be observed in the white adipocytes differentiated from

primary pre-adipocytes of the subcutaneous adipose tissue of mice (Supporting Information, Figure S5).

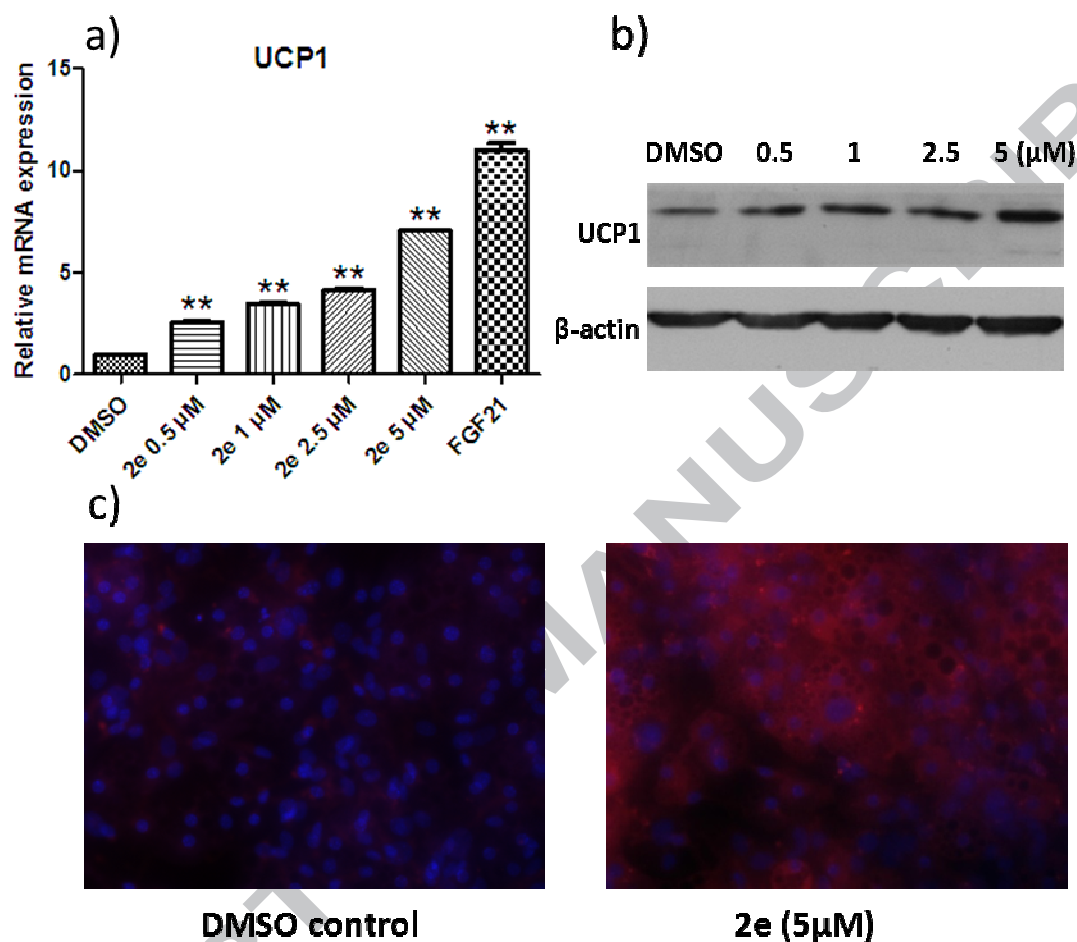


**Figure 5.** Compound **2e** induces browning of white adipose *in vitro*. a) **2e** enhances the expression level of UCP1 in a dose-dependent manner in a real-time PCR assay. FGF21 (1  $\mu$ g/mL) was used as a positive control. b) **2e** increases the level of UCP1 protein as determined by a western blot assay. The UCP1 protein was found to be 33 kDa in size. c) Representative images from immunofluorescence against UCP1. Results are the mean ( $\pm$  SEM) or representative of three independent experiments (\*\*P < 0.01).

One of the most significant features in brown fat development is mitochondrial biogenesis and remodelling.<sup>7</sup> Consequently, we further evaluated the effect of **2e** on mitochondrial biogenesis by assessing the expression of several mitochondria-related genes including PGC-1 $\alpha$  (Peroxisome proliferator-activated receptor- $\gamma$  coactivator 1 $\alpha$ ), CS (Citrate Synthase), CPT1 (Carnitine Palmytoyltransferase-1) and COXII (Cytochrome c Oxidase subunit II),<sup>11c, 19, 21</sup> and found that **2e** significantly improves the mRNA levels of these genes. More significantly, the protein level of SDH (Succinate Dehydrogenase)<sup>19</sup>, an important mitochondrial function protein, is also increased (Figure 6). The role of compound **2e** in the induction of mitochondrial biogenesis was further supported by electron microscopic analysis (SI, Figure S6).

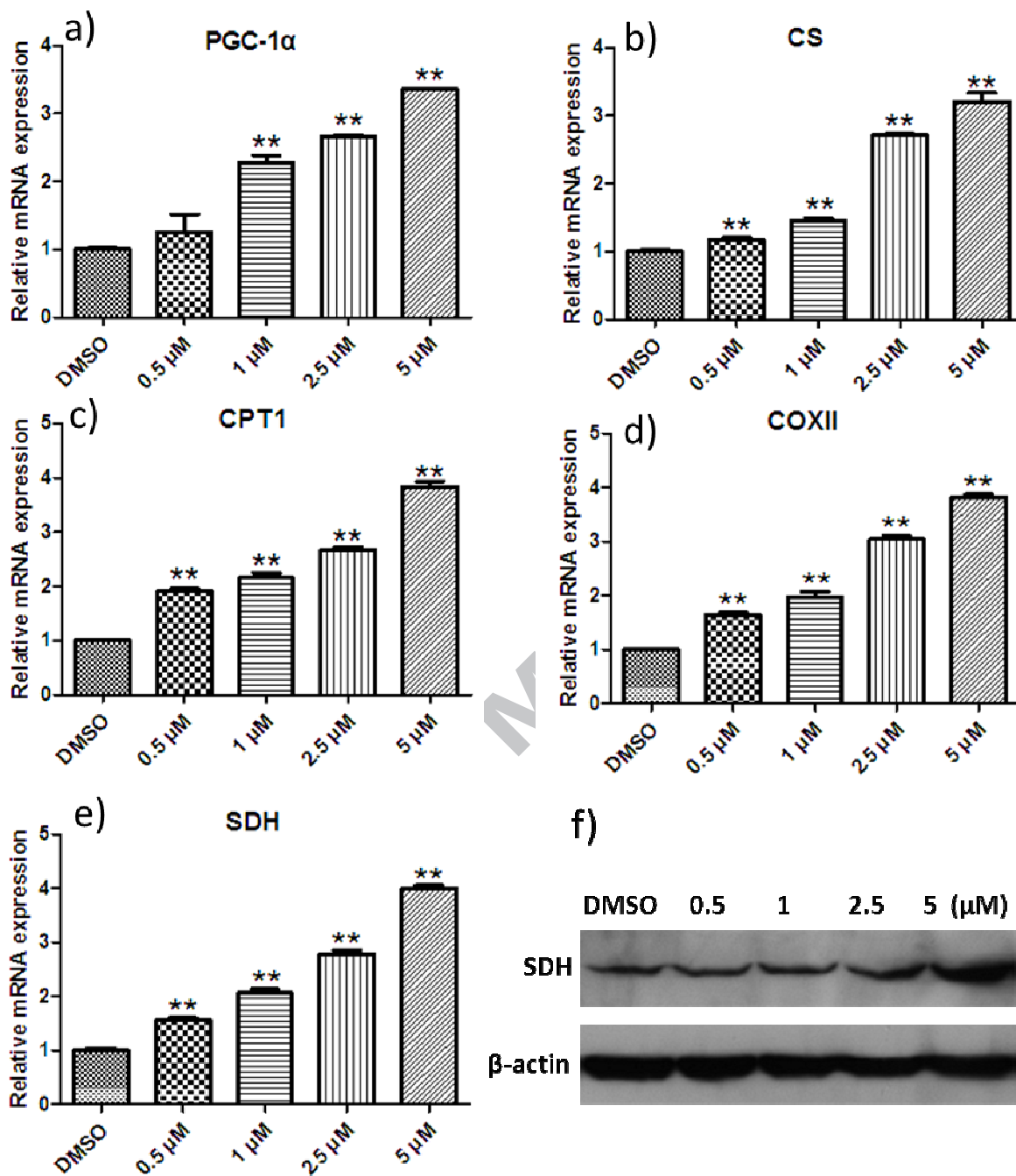


**Figure 6.** Compound **2e** promotes expression of mitochondrial genes. a-e) **2e** induces the mRNA levels of PGC-1 $\alpha$ , CS, CPT1, COXII and SDH in a real-time PCR assay. (f) **2e** elevates the protein level of SDH as determined by western blot analysis. SDH protein was found to be 70

kDa in size. Results are the mean ( $\pm$  SEM) or representative of three independent experiments (\*\* $P < 0.01$ ).

The *in vivo* adipose browning effect of **2e** was also investigated in a mouse model. Similar to the *in vitro* investigation, repeated oral administration of **2e** at 20 mg/kg/day induced UCP1 elevation in mouse subcutaneous white adipose tissue (Supporting Information, Figure S7). The *in vivo* browning effect of **2e** was further confirmed in an immunohistochemistry assay where a robust increase in the UCP1-positive stained area of subcutaneous white adipose tissue was observed (Figure 7). It was also noteworthy that compound **2e** caused a similar increase in UCP1 in mouse interscapular brown adipose tissues, suggesting its potential to improve the biological functions of BAT (Supporting Information, Figure S8).

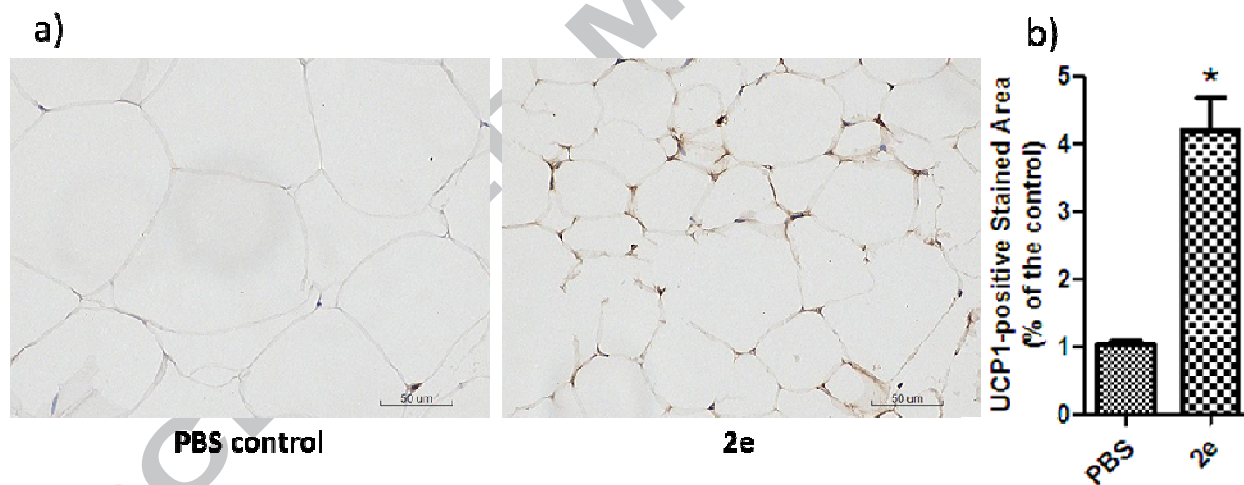


**Figure 7.** Compound **2e** induces browning of the subcutaneous white adipose tissue *in vivo* in mice. a) Representative images of immunohistochemistry against UCP1. b) The quantitative ratio of the UCP1-positive stained area. Results are the mean ( $\pm$  SEM) or representative of two independent experiments (\* $p < 0.05$ ).

In summary, we have designed and synthesized a series of 1-benzyl-4-phenyl-1*H*-1,2,3-triazole derivatives as novel small molecules that improve the transcriptional functions of ERR $\gamma$ . One of the most promising compounds **2e** directly binds with ERR $\gamma$ -LBD and potently stimulates the adipose browning process both *in vitro* and *in vivo*. Compound **2e** also significantly improves mitochondrial biogenesis and the biological functions in MEF-differentiated white adipocytes although a detailed mechanism is yet to be confirmed. Our studies suggest that compound **2e** has excellent potential to serve as a lead compound for the development of new therapeutic agents for the treatment of obesity and related disorders.

## EXPERIMENTAL SECTION

**General Methods for Chemistry.** All reagents and solvents used as were purchased from commercial sources. Flash chromatography was performed using silica gel (300 mesh). All reactions were monitored by TLC, using silica gel plates with fluorescence F254 and UV light visualization. <sup>1</sup>H NMR and <sup>13</sup>C NMR spectra were recorded on a Bruker AV-400 spectrometer at 400MHz and Bruker AV-500 spectrometer at 125 MHz. Coupling constants (*J*) are expressed in hertz (Hz). Chemical shifts ( $\delta$ ) of NMR are reported in parts per million (ppm) units relative to an internal control (TMS). High resolution ESI-MS were recorded on an Applied Biosystems Q-STAR Elite ESI-LC-MS/MS mass spectrometer. The purity of compounds was determined by reverse-phase high performance liquid chromatography (HPLC) analysis to be >95%. HPLC instrument: Dionex Summit HPLC (Column: Diamonsil C18, 5.0  $\mu$ m, 4.6  $\times$  250mm (Dikma Technologies); detector: PDA-100 photodiode array; injector: ASI-100 autoinjector; pump: p-680A). A flow rate of 1.0 mL/min was used with mobile phase of MeOH in H<sub>2</sub>O with 0.1% modifier (ammonia or trifluoroacetic acid e, v/v).

**2-(4-Bromophenoxy)tetrahydro-2H-pyran (4a).** General procedure for the synthesis of **4a-k**. 3,4-Dihydro-2H-pyran (4.0 mL, 43.4 mmol) was added to a solution of 4-bromophenol (5 g, 28.9 mmol) in anhydrous CH<sub>2</sub>Cl<sub>2</sub> (100 mL) under argon, followed by pyridinium *p*-toluenesulfonate (75 mg, 0.3 mmol). The reaction mixture was stirred at room temperature overnight. The crude reaction mixture was washed three times with saturated aqueous NaHCO<sub>3</sub> and brine, dried with Na<sub>2</sub>SO<sub>4</sub>, filtered, and concentrated in vacuo. The resultant crude material was purified by column chromatography (SiO<sub>2</sub>, PE/EtOAc, 10:1) to give the title compound (7.3g, 98% yield). <sup>1</sup>H NMR (400 MHz, CDCl<sub>3</sub>) δ 7.37 (d, *J* = 8.8 Hz, 2H), 6.94 (d, *J* = 8.8 Hz, 2H), 5.37 (t, *J* = 3.0 Hz, 1H), 3.90-3.84 (m, 1H), 3.62-3.57 (m, 1H), 2.05-1.94 (m, 1H), 1.87-1.83 (m, 2H), 1.74-1.59 (m, 3H).

**2-(4-Ethynylphenoxy)tetrahydro-2H-pyran (5a).** General procedure for the synthesis of **5a-k**. To a solution of **4a** (1g, 3.9 mmol), PdCl<sub>2</sub>(PPh<sub>3</sub>)<sub>2</sub> (55 mg, 0.078 mmol) and CuI (7.4 mg, 0.040 mmol) were added trimethylsilylacetylene (572 mg, 5.84 mmol) with syringe under argon. After the reaction mixture was stirred at 80°C overnight, it was diluted with CH<sub>2</sub>Cl<sub>2</sub> (50 mL) and filtered through a pad of Celite. The filtrate was diluted with H<sub>2</sub>O, and extracted several times with CH<sub>2</sub>Cl<sub>2</sub>. The combined organic extracts were washed with brine, dried over anhydrous Na<sub>2</sub>SO<sub>4</sub>, filtered, and concentrated in vacuo. The residue was dissolved in methanol (150 mL), followed by adding K<sub>2</sub>CO<sub>3</sub> (978 mg, 7.09 mmol). The reaction mixture was stirred at room temperature for 4 h, and concentrated in vacuo. The residue was diluted with H<sub>2</sub>O, and extracted several times with CH<sub>2</sub>Cl<sub>2</sub>. The combined organic phases were washed with brine and dried over anhydrous Na<sub>2</sub>SO<sub>4</sub>. Filtration and removal of the solvent gave a crude oil that was subjected to column chromatography (SiO<sub>2</sub>, PE/EtOAc, stepwise elution, PE to 10:1) to give the title product. (759 mg, 97% yield). <sup>1</sup>H NMR (400 MHz, CDCl<sub>3</sub>) δ 7.42 (d, *J* = 8.8 Hz, 2H), 6.99 (d, *J* = 8.8

Hz, 2H), 5.43 (t,  $J = 3.2$  Hz, 1H), 3.90-3.84 (m, 1H), 3.64-3.58 (m, 1H), 2.99 (s, 1H), 2.04-1.95 (m, 1H), 1.88-1.84 (m, 2H), 1.74-1.59 (m, 3H).

**1-(4-Isopropylbenzyl)-4-(4-(tetrahydro-2H-pyran-2-yloxy)phenyl)-1H-1,2,3-triazole (6a).** General procedure for the synthesis of **6a-k**. Sodium ascorbate (60 mg, 0.3 mmol) and  $\text{CuSO}_4$  (16 mg, 0.1 mmol) were added to a solution of **5a** (202 mg, 1 mmol) and 1-(azidomethyl)-4-isopropylbenzene (193 mg, 1.1 mmol) in 1:1 *t*-BuOH/ $\text{H}_2\text{O}$  (20 mL). The reaction mixture was stirred at room temperature under argon overnight and then was concentrated in vacuo, diluted with  $\text{H}_2\text{O}$ , and extracted with  $\text{CH}_2\text{Cl}_2$ . The combined organic phases were dried over anhydrous  $\text{Na}_2\text{SO}_4$ , filtered, and concentrated in vacuo. The residue was subjected to column chromatography ( $\text{SiO}_2$ , PE/EtOAc, 5:1) to give the title compound (147 mg, 40% yield).  $^1\text{H}$  NMR (400 MHz,  $\text{CDCl}_3$ )  $\delta$  7.71 (d,  $J = 8.4$  Hz, 2H), 7.57 (s, 1H), 7.24 (s, 4H), 7.08 (d,  $J = 8.8$  Hz, 2H), 5.52 (s, 2H), 5.44 (t,  $J = 3.2$  Hz, 1H), 3.93-3.87 (m, 1H), 3.63-3.58 (m, 1H), 2.96-2.86 (m, 1H), 2.07-1.96 (m, 1H), 1.88-1.85 (m, 2H), 1.71-1.59 (m, 3H), 1.24 (d,  $J = 7.2$  Hz, 6H).

**4-(1-(4-Isopropylbenzyl)-1H-1,2,3-triazol-4-yl)phenol (2a).** General procedure for the synthesis of **2a-k**. Pyridinium *p*-toluenesulfonate (5 mg, 0.02 mmol) was added to a solution of **6a** (147 mg, 0.39 mmol) in EtOH (20 mL). The reaction mixture was then warmed to 50 °C and stirred for 2 h. After the complete consumption of the starting material, the solution was concentrated in vacuo and subjected to flash column chromatography ( $\text{SiO}_2$ ,  $\text{CH}_2\text{Cl}_2/\text{EtOAc}$ , 10:1) to give the title compound (106 mg, 90% yield, white solid).  $^1\text{H}$  NMR (400 MHz,  $\text{DMSO}-d_6$ )  $\delta$  9.55 (s, 1H), 8.42 (s, 1H), 7.63 (d,  $J = 8.8$  Hz, 2H), 7.28-7.23 (m, 4H), 6.81 (d,  $J = 8.8$  Hz, 2H), 5.55 (d, 2H), 2.90-2.83 (m, 1H), 1.17 (d,  $J = 7.2$  Hz, 6H).  $^{13}\text{C}$  NMR (125 MHz,  $\text{DMSO}-d_6$ )  $\delta$  157.21, 148.34, 146.93, 133.53, 127.90, 126.63, 126.53, 121.69, 120.00, 115.55, 52.70, 33.10,

23.76. HRMS (ESI) for  $C_{18}H_{19}N_3O$   $[M + H]^+$ , calcd: 294.1601. Found: 294.1598. HPLC analysis: MeOH-H<sub>2</sub>O (78:22) with 0.1% ammonia, 6.39 min, 97.17% purity.

**1-(4-Isopropylbenzyl)-4-phenyl-1H-1,2,3-triazole (2b).** <sup>1</sup>H NMR (400 MHz, DMSO-*d*<sub>6</sub>)  $\delta$  8.62 (s, 1H), 7.84 (d,  $J = 7.6$  Hz, 2H), 7.43 (t,  $J = 7.6$  Hz, 2H), 7.33 (d,  $J = 7.6$  Hz, 1H), 7.30-7.24 (m, 4H), 5.59 (s, 2H), 2.92-2.82 (m, 1H), 1.17 (d,  $J = 7.2$  Hz, 6H). <sup>13</sup>C NMR (125 MHz, DMSO-*d*<sub>6</sub>)  $\delta$  148.39, 146.59, 133.39, 130.65, 128.82, 127.93, 127.81, 126.65, 125.10, 121.40, 52.79, 33.09, 23.74. HRMS (ESI) for  $C_{18}H_{19}N_3$   $[M + H]^+$ , calcd: 278.1652. Found: 278.1650. HPLC analysis: MeOH-H<sub>2</sub>O (78:22) with 0.1% ammonia, 10.68 min, 95.12% purity.

**2-(1-(4-Isopropylbenzyl)-1H-1,2,3-triazol-4-yl)phenol (2c).** <sup>1</sup>H NMR (400 MHz, DMSO-*d*<sub>6</sub>)  $\delta$  10.17 (s, 1H), 8.45 (s, 1H), 8.00 (dd,  $J = 1.6, 7.6$  Hz, 1H), 7.28 (d,  $J = 8.4$  Hz, 2H), 7.24 (d,  $J = 8.0$  Hz, 2H), 7.18-7.13 (m, 1H), 6.95 (d,  $J = 8.0$  Hz, 1H), 6.89 (t,  $J = 7.4$  Hz, 1H), 5.62 (s, 2H), 2.92-2.81 (m, 1H), 1.17 (d,  $J = 6.8$  Hz, 6H). <sup>13</sup>C NMR (125 MHz, DMSO-*d*<sub>6</sub>)  $\delta$  153.80, 148.32, 143.12, 133.60, 128.61, 127.94, 126.61, 126.43, 123.19, 119.24, 116.94, 115.92, 52.53, 33.09, 23.75. HRMS (ESI) for  $C_{18}H_{19}N_3O$   $[M + H]^+$ , calcd: 294.1601. Found: 294.1599. HPLC analysis: MeOH-H<sub>2</sub>O (78:22) with 0.1% ammonia, 9.90 min, 96.42% purity.

**3-(1-(4-Isopropylbenzyl)-1H-1,2,3-triazol-4-yl)phenol (2d).** <sup>1</sup>H NMR (400 MHz, DMSO-*d*<sub>6</sub>)  $\delta$  9.52 (s, 1H), 8.56 (s, 1H), 7.29-7.19 (m, 7H), 6.73-6.70 (m, 1H), 5.57 (s, 2H), 2.92-2.81 (m, 1H), 1.17 (d,  $J = 6.8$  Hz, 6H). <sup>13</sup>C NMR (125 MHz, DMSO-*d*<sub>6</sub>)  $\delta$  157.69, 148.37, 146.67, 133.43, 131.84, 129.86, 127.93, 126.64, 121.35, 116.01, 114.86, 111.82, 52.75, 33.10, 23.75. HRMS (ESI) for  $C_{18}H_{19}N_3O$   $[M + H]^+$ , calcd: 294.1601. Found: 294.1598. HPLC analysis: MeOH-H<sub>2</sub>O (78:22) with 0.1% ammonia, 6.90 min, 98.01% purity.

**4-(1-(4-Isopropylbenzyl)-1H-1,2,3-triazol-4-yl)benzene-1,2-diol (2e).** <sup>1</sup>H NMR (400 MHz, DMSO-*d*<sub>6</sub>)  $\delta$  9.02 (s, 2H), 8.38 (s, 1H), 7.28-7.23 (m, 5H), 7.06 (dd,  $J = 1.6, 8.0$  Hz, 1H), 6.76

(d,  $J = 8.0$  Hz, 1H), 5.53 (s, 2H), 2.91-2.81 (m, 1H), 1.17 (d,  $J = 6.8$  Hz, 6H).  $^{13}\text{C}$  NMR (125 MHz, DMSO- $d_6$ )  $\delta$  148.32, 147.07, 145.46, 145.30, 133.55, 127.90, 126.61, 122.13, 120.01, 116.59, 115.87, 112.67, 52.66, 33.10, 23.76. HRMS (ESI) for  $\text{C}_{18}\text{H}_{19}\text{N}_3\text{O}_2$   $[\text{M} + \text{H}]^+$ , calcd: 310.1550. Found: 310.1549. HPLC analysis: MeOH- $\text{H}_2\text{O}$  (65:35) with 0.1% trifluoroacetic acid, 12.68 min, 96.90% purity.

**4-(1-(3-Isopropylbenzyl)-1H-1,2,3-triazol-4-yl)benzene-1,2-diol (2f).**  $^1\text{H}$  NMR (400 MHz, DMSO- $d_6$ )  $\delta$  9.03 (s, 2H), 8.39 (s, 1H), 7.31-7.20 (m, 4H), 7.12-7.06 (m, 2H), 6.76 (d,  $J = 8.4$  Hz, 1H), 5.56 (s, 2H), 2.92-2.82 (m, 1H), 1.18 (d,  $J = 7.2$  Hz, 6H).  $^{13}\text{C}$  NMR (125 MHz, DMSO- $d_6$ )  $\delta$  148.91, 147.04, 145.47, 145.32, 136.04, 128.72, 125.97, 125.91, 125.26, 122.11, 120.10, 116.60, 115.87, 112.68, 52.97, 33.29, 23.77. HRMS (ESI) for  $\text{C}_{18}\text{H}_{19}\text{N}_3\text{O}_2$   $[\text{M} + \text{H}]^+$ , calcd: 310.1550. Found: 310.1549. HPLC analysis: MeOH- $\text{H}_2\text{O}$  (65:35) with 0.1% trifluoroacetic acid, 11.83 min, 98.27% purity.

**4-(1-(2-Isopropylbenzyl)-1H-1,2,3-triazol-4-yl)benzene-1,2-diol (2g).**  $^1\text{H}$  NMR (400 MHz, DMSO- $d_6$ )  $\delta$  9.02 (s, 2H), 8.27 (s, 1H), 7.38-7.31 (m, 2H), 7.25-7.15 (m, 3H), 7.08-7.05 (m, 1H), 6.75 (d,  $J = 8.4$  Hz, 1H), 5.65 (s, 2H), 3.36-3.30 (m, 1H), 1.12 (d,  $J = 6.8$  Hz, 6H).  $^{13}\text{C}$  NMR (125 MHz, DMSO- $d_6$ )  $\delta$  146.91, 146.87, 145.47, 145.31, 132.51, 129.25, 128.72, 125.99, 125.65, 122.10, 120.05, 116.60, 115.86, 112.68, 50.59, 28.03, 23.55. HRMS (ESI) for  $\text{C}_{18}\text{H}_{19}\text{N}_3\text{O}_2$   $[\text{M} + \text{H}]^+$ , calcd: 310.1550. Found: 310.1551. HPLC analysis: MeOH- $\text{H}_2\text{O}$  (85:15) with 0.1% trifluoroacetic acid, 3.88 min, 96.48% purity.

**4-(1-Benzyl-1H-1,2,3-triazol-4-yl)benzene-1,2-diol (2h).**  $^1\text{H}$  NMR (400 MHz, DMSO- $d_6$ )  $\delta$  9.03 (s, 2H), 8.38 (s, 1H), 7.40-7.32 (m, 5H), 7.25 (d,  $J = 1.6$  Hz, 1H), 7.07 (dd,  $J = 2.0, 8.0$  Hz, 1H), 6.76 (d,  $J = 8.4$  Hz, 1H), 5.59 (s, 2H).  $^{13}\text{C}$  NMR (125 MHz, DMSO- $d_6$ )  $\delta$  147.07, 145.46, 145.32, 136.12, 128.71, 128.04, 127.80, 122.09, 120.12, 116.59, 115.87, 112.67, 52.84. HRMS

(ESI) for  $C_{15}H_{13}N_3O_2$   $[M + H]^+$ , calcd: 268.1081. Found: 268.1079. HPLC analysis: MeOH-H<sub>2</sub>O (65:35) with 0.1% trifluoroacetic acid, 5.00 min, 95.06% purity.

**4-(1-(4-Methylbenzyl)-1H-1,2,3-triazol-4-yl)benzene-1,2-diol (2i).** <sup>1</sup>H NMR (400 MHz, DMSO-*d*<sub>6</sub>) δ 9.02 (s, 2H), 8.34 (s, 1H), 7.25-7.17 (m, 5H), 7.06 (dd, *J* = 0.8, 8.0 Hz, 1H), 6.76 (d, *J* = 8.0 Hz, 1H), 5.53 (s, 2H), 2.28 (s, 3H). <sup>13</sup>C NMR (125 MHz, DMSO-*d*<sub>6</sub>) δ 147.04, 145.46, 145.30, 137.38, 133.12, 129.24, 127.86, 122.13, 119.97, 116.58, 115.87, 112.67, 52.66, 20.65. HRMS (ESI) for  $C_{16}H_{15}N_3O_2$   $[M + H]^+$ , calcd: 282.1237. Found: 282.1236. HPLC analysis: MeOH-H<sub>2</sub>O (65:35) with 0.1% ammonia, 6.71 min, 95.57% purity.

**4-(1-(4-Tert-butylbenzyl)-1H-1,2,3-triazol-4-yl)benzene-1,2-diol (2j).** <sup>1</sup>H NMR (400 MHz, DMSO-*d*<sub>6</sub>) δ 9.03 (s, 2H), 8.37 (s, 1H), 7.39 (d, *J* = 8.4 Hz, 2H), 7.28-7.25 (m, 3H), 7.08-7.05 (m, 1H), 6.76 (d, *J* = 8.4 Hz, 1H), 5.54 (s, 2H), 1.25 (s, 9H). <sup>13</sup>C NMR (125 MHz, DMSO-*d*<sub>6</sub>) δ 150.54, 147.07, 145.46, 145.30, 133.19, 127.62, 125.47, 122.12, 120.02, 116.59, 115.86, 112.66, 52.57, 34.23, 31.01. HRMS (ESI) for  $C_{19}H_{21}N_3O_2$   $[M + H]^+$ , calcd: 324.1707. Found: 324.1706. HPLC analysis: MeOH-H<sub>2</sub>O (85:15) with 0.1% trifluoroacetic acid, 4.40 min, 96.70% purity.

**4-(1-(Biphenyl-4-ylmethyl)-1H-1,2,3-triazol-4-yl)benzene-1,2-diol (2k).** <sup>1</sup>H NMR (400 MHz, DMSO-*d*<sub>6</sub>) δ 9.04 (s, 2H), 8.43 (s, 1H), 7.69-7.64 (m, 4H), 7.48-7.41 (m, 4H), 7.38-7.34 (m, 1H), 7.26 (d, *J* = 2.0 Hz, 1H), 7.08 (dd, *J* = 2.0, 8.4 Hz, 1H), 6.77 (d, *J* = 8.0 Hz, 1H), 5.64 (s, 2H). <sup>13</sup>C NMR (125 MHz, DMSO-*d*<sub>6</sub>) δ 147.12, 145.48, 145.33, 139.95, 139.56, 135.27, 128.90, 128.44, 127.55, 127.03, 126.65, 122.10, 120.16, 116.61, 115.88, 112.69, 52.54. HRMS (ESI) for  $C_{21}H_{17}N_3O_2$   $[M + H]^+$ , calcd: 344.1394. Found: 344.1390. HPLC analysis: MeOH-H<sub>2</sub>O (65:35) with 0.1% ammonia, 14.09 min, 95.61% purity.

**Computational Protein-Ligand Docking.** The published crystal structure of ERRγ with compound **1** (PDB: 2GPP) was used for the modelling of possible binding modes. All

crystallographic water molecules were deleted except two water molecules which mediate the hydrogen bonds between **1** and ERR $\gamma$ . The crystal structure was prepared for docking using the protein preparation wizard in Maestro (Version 9.6, Schrödinger), which assigns bond orders, adds hydrogens and missing atoms. The active site was defined by manually selecting the original ligand and using the default of box length with a Receptor Grid Generation model. Glide was used for the protein-ligand docking in an XP protocol. Multiple stereoisomers, ionization states, and 3D structures of each ligand as the input to the docking calculation, were initially generated by LigPrep using the OPLS\_2005 force field. Docked binding modes were ranked using the Docking Score and manually inspected for a reasonable interaction. All docking figures were generated using PyMOL (Schrödinger, USA).

**Cell Lines and Cell Culture.** The human 293FT cell line was purchased from Invitrogen. Cells were grown in the medium recommended by Invitrogen, and cultured in a complete medium containing 10% FBS in a 5% CO<sub>2</sub> incubator at 37°C.

**Primary mouse embryonic fibroblast (MEF).** MEF were harvested, according to the standard protocol.<sup>22</sup> Briefly, uteri were obtained at E13.5 days of pregnancy and embryos were isolated. Heads and viscera were removed and the remaining bodies were washed in PBS, transferred to 10 cm petridishes and minced with a pair of scissors before being digested with 0.1% trypsin (GIBCO) for 40min at 37°C. Following digestion, the suspension was centrifuged at 1000 g for 5 min, then 10 mL DMEM (Hyclone), supplemented with 10% FBS (Hyclone) and 1% P/S (Hyclone), was added and the tissue pipetted up and down to get a single cell suspension. MEF were cultured in 10 cm cell culture dishes until 80–85% confluent and then were passaged at a ratio of 1: 2.

**Isolation of preadipocytes from adipose tissues.** Isolation of stromal cells from fat tissue was performed as previously described.<sup>6, 23</sup> Subcutaneous fat was dissected out, rinsed in PBS, minced, and digested for 40 min at 37 °C in 0.1% (w/v) collagenase solution (Collagenase type I, dissolved in D-Hanks buffer). The digested tissue was filtered through a 100 µm nylon mesh to remove undigested tissues before being centrifuged at 1000 g for 5 min. The pellet (preadipocytes) was collected and washed again in PBS, then 5 mL DMEM, supplemented with 15% FBS and 1% P/S, was added and the tissue pipetted up and down to get a single cell suspension. The cells were cultured in 4cm cell culture dishes and the cell medium was changed every day.

For white adipocyte differentiation assays, MEF and preadipocytes from subcutaneous adipose tissue were plated in 6 well plates and cultured in DMEM with 10 % FBS. Two days after reaching confluence (day 0), differentiation was induced by incubation of the cells in differentiation medium containing 5 µg/mL insulin (Sigma), 1 µM dexamethasone (Sigma), and 0.5 mM isobutylmethylxanthine (Sigma). After 2 days, the media was replaced with DMEM supplemented with 10% FBS, 5 µg/ml insulin and 1µM rosiglitazone, and the cells were re-fed every 2 days until day 8. Compounds **2e** and **2c** were dissolved in demethylsulfoxide (DMSO) and FGF21 was dissolved in PBS for cell culture studies. At day 8, cells were exposed to compounds at the concentrations indicated with DMEM supplemented with 10% FBS for additional two days.

**Transient Transfection Mammalian Two-hybrid Reporter Gene Assay.** 293FT cells were seeded in 96-well plate at a density of 10,000 cells/well in DMEM containing 10% FBS. After plating for 18-24 hrs, transient transfections were performed with Lipofectamine 2000 (Invitrogen) according to the manufacturer's instructions. Total DNA for transfections included

GAL4-DBD-ERR $\gamma$ -LBD vector (0.5 ng), pcDNA-PGC-1 $\alpha$  vector (0.5 ng), pFR vector (25 ng), and internal control vector pRLTK renilla (3 ng). After cells were transfected for 6 h, 2  $\mu$ M of the test compounds were then added for an additional 24 hrs. (When the concentration of test compounds was up to 10  $\mu$ M or higher, the luciferase light units of both the firefly luciferase and renilla luciferase groups were significantly reduced, which may be caused by the toxicity of these compounds against the 293FT cells at such high concentration. Therefore, the concentration of these compounds was set to a relative low value of 2  $\mu$ M.) Luciferase activity was measured by dual luciferase reporter assay system (Promega) according to the manufacturer's instruction on a Veritas Microplate Luminometer. Relative luciferase light units (RLU) were the ratio of the absolute activity of firefly luciferase to that of renilla luciferase. The experiment was done in triplicate, and results are representatives of at least three independent experiments.

**Real-Time PCR Assay.** Total RNA was isolated from cells and tissues using Trizol Reagent (Invitrogen). First-strand cDNA synthesis was performed with Superscript<sup>TM</sup> III Reverse Transcriptase (Invitrogen). Quantification of mRNA levels was performed using SYBR<sup>®</sup> Premix Ex Taq<sup>TM</sup> (TaKaRa) under optimized conditions following the manufacturer's instruction. The reference gene chosen was GAPDH. The primers were synthesized by Invitrogen in Shanghai, China.

**Western Blot Assay.** Cells were washed twice with ice-cold PBS and lysed with RIPA buffer (Beyotime) for 30 min on ice. Cell lysates were centrifuged at 12,000 g for 15 min at 4 $^{\circ}$ C and supernatants were collected. 40  $\mu$ g of cellular proteins were resolved by 12% SDS-PAGE gel and transferred to PVDF membrane (Millipore). The membranes were probed overnight with specific antibodies at 4 $^{\circ}$ C, washed three times with TBST followed by incubation with rabbit radish

peroxidase conjugated secondary antibody for 4 h at 4°C. The membranes were developed by applying ECL Plus developing system (GE Healthcare). Membranes were stripped with stripping buffer (Comwin biotech) and reprobbed with other antibodies if necessary. The primary antibodies used in this experiment are UCP1 (1:1000; abcam; ab10983); SDH (1:4000; epitomics; p31040); MCAD (1:5000; epitomics; P11310); ATP5b (1:1000; abcam; ab150291);  $\beta$ -actin (1:2000; abcam; ab8227).

**Immunofluorescence Staining Assay.** For immunofluorescence staining, coverslips plated with white adipocyte derived MEF cells were fixed in 4% formaldehyde and were blocked with 5% bovine serum albumin (BSA) in PBS at room temperature for 1 h and then incubated with rabbit anti-UCP1 antibody (1:1000; Abcam; ab10983) at 4°C overnight. Then the sections were incubated with Alexa Fluor 647-conjugated anti-rabbit secondary antibody (1:200; Abcam; ab150079) at room temperature for 1 h before the nuclei were stained by DAPI. Coverslips were mounted onto glass slides. Labeled samples were imaged using Leica microscope.

**Electron Microscopy Detection.** At day 10 the white adipose cells differentiated from MEF were washed 3 times in PBS, fixed for 1 hour with 2.5% glutaraldehyde, and postfixed for 1 hour with 1% osmic acid. After dehydration in a graded series of cold ethanol, cells were subsequently embedded in epoxy resin. Ultrafine sections were performed, using an ultramicrotome, before staining with uranyl acetate and counterstaining with lead citrate. Sections were then examined with a transmission electron microscope (Hitachi-600; Hitachi Ltd, Tokyo, Japan).

**Animal Study.** Male mice (8 weeks old) in C57BL6 background were housed in SPF mice room and maintained on a 12 h light-dark cycle at 23°C and fed a high-fat diet (21.9 kJ/g, 60%

of energy as fat, 20% of energy as protein, 20% of energy as carbohydrate; D12492; Research Diet, New Brunswick, NJ, USA) for 4 weeks. At the same time mice were given **2e** (20 mg/kg body weight) or vehicle (5% alcohol in PBS) every day, by oral gavage. The animals were killed 4 weeks later, and tissues were isolated and kept in  $-80^{\circ}\text{C}$  for RNA extraction or fixed in 4% formaldehyde for morphology.

**Immunohistochemistry Assay.** White adipose tissues and brown adipose tissues were fixed in 4% formaldehyde overnight at room temperature immediately after the mice were sacrificed. Tissues were paraffinized and sectioned by microtome. Paraffin embedded sections of adipose tissues were stained with anti-rabbit UCP1 (1:1000; Abcam; ab10983) to assess the expression of UCP1. Sections were examined by light microscopy.

**Cloning, protein expression and purification.** The gene encoding ERR $\gamma$  229-458 amino acids was cloned in pET15b. The target protein was expressed with an *N*-terminal hexahistidine tag and a thrombin cleavage site. *E. coli* BL21 (DE3) cells transformed with expression plasmids were grown in Luria-Bertani (LB) medium to an OD<sub>600nm</sub> of 0.6-0.8 at 310 K. Expression of the recombinant proteins was induced with 0.3 mM isopropyl  $\beta$ -D-1-thiogalactopyranoside (IPTG) and the cells were further grown for 20 h at 289 K. The target protein was first purified from a nickel-nitrilotriacetic acid (Ni-NTA) affinity column (Qiagen) in an eluting buffer containing 25 mM Tris-HCl, pH 8.0, 150 mM NaCl, 200 mM imidazole. Further purification was then achieved by anion exchange chromatography (Source Q, GE healthcare) and gel filtration (Hiload 16/60 Superdex 75 size exclusion column, GE Healthcare) equilibrated against a phosphate buffer at pH8.0.

**Isothermal Titration Calorimetry (ITC).** Isothermal titration calorimetry experiments were performed using a MicroCal iTC200 (GE Healthcare) at 20 °C. The protein eluted from gel

filtration was concentrated by ultrafiltration (Millipore Amicon) and supplemented with dimethyl sulfoxide (DMSO) to a final concentration of 0.24%. Small molecules were diluted in the same buffer from 50 mM stock in DMSO. All solutions were degassed before titrations were performed. The sample cell was filled with 200  $\mu$ L small molecule in 122  $\mu$ M and the syringe was filled with 60  $\mu$ L protein in 1.36 mM. The titration consisted of an initial injection of 0.5  $\mu$ L followed by 19 injections of 2  $\mu$ L. To determine the baseline, the protein was titrated into the same buffer without the small molecules under the same conditions. Data was analyzed with the software Origin 7.0 (OriginLab) using the one set of sites model.

**Circular dichroism (CD) Spectroscopy.** CD experiments were carried out on a circular dichroism spectrometer (Chirascan, Applied Photophysics Ltd.). Purified protein in phosphate buffer was diluted to 0.2 mg/mL. The ligands were dissolved in DMSO to 200 mM before being added to the protein solution and incubated overnight. Measurements were made using a quartz cuvette with 1 mm path length. For thermal sensitivity experiments, ellipticity from 200 nm to 260 nm was measured at one-degree increments of the temperature from 30 °C to 60 °C.

#### ASSOCIATED CONTENT

**Supporting Information.** Experimental procedures, characterization data, biological data, and copies of  $^1\text{H}$  NMR and  $^{13}\text{C}$  NMR spectra for compounds **2a-k**. This material is available free of charge via the Internet.

#### AUTHOR INFORMATION

##### Corresponding Author

\*Tel: +86-20-32015276. Fax: +86-20-32015299. E-mail: ding\_ke@gibh.ac.cn,

[wu\\_donghai@gibh.ac.cn](mailto:wu_donghai@gibh.ac.cn), [ren\\_xiaomei@gibh.ac.cn](mailto:ren_xiaomei@gibh.ac.cn)

## Author Contributions

<sup>#</sup>These authors contributed equally.

## Notes

The authors declare no competing financial interests.

## ACKNOWLEDGMENT

We thank the Strategic Collaboration grant between China and New Zealand from Ministry of Science and Technology of China (#2014DFG32100), National Basic Research Program of China (2011CB504004 and 2010CB94550), the National Natural Science Foundation (#81425021, #21272235), 100-Distinguished Scientist Award of Guangdong province (Nanyue-Baijie award) and the Key Project on Innovative Drug of Guangdong Province (#2012A080201014).

## ABBREVIATIONS

ERR: estrogen-related receptor, WAT: white adipose tissue, BAT: brown adipose tissue, PET: positron-emission-tomography, FGF21: fibroblast growth factor 21, MOA: mechanisms of action, UCP1: uncoupling protein 1, SHP: small heterodimer partner, ATP5b: ATP synthase 5b, MCAD: medium-chain acyl-coenzyme A dehydrogenase, MEF: mouse embryonic fibroblasts, Prdm16: PR domain containing 16, PGC-1 $\alpha$ : peroxisome proliferator-activated receptor- $\gamma$  coactivator 1, CS: citrate synthase, CPT1: carnitine palmytoyltransferase-1, COXII: cytochrome C oxidase subunit II, SDH: succinate dehydrogenase, ITC: Isothermal Titration Calorimetry, CD: Circular dichroism Spectroscopy, LBD: ligand binbding domain, T<sub>m</sub>: melting temperature.

## REFERENCES

1. Farmer, S. R. Molecular determinants of brown adipocyte formation and function. *Genes Dev.* **2008**, *22*, 1269-1275.
2. Gesta, S.; Tseng, Y.-H.; Kahn, C. R. Developmental Origin of Fat: Tracking Obesity to Its Source. *Cell* **2007**, *131*, 242-256.
3. (a) Cannon, B.; Nedergaard, J. Brown Adipose Tissue: Function and Physiological Significance. *Physiol. Rev.* **2004**, *84*, 277-359. (b) Bonet, M. L.; Oliver, P.; Palou, A. Pharmacological and nutritional agents promoting browning of white adipose tissue. *Biochim. Biophys. Acta* **2013**, *1831*, 969-985. (c) Kopecky, J.; Clarke, G.; Enerback, S.; Spiegelman, B.; Kozak, L. P. Expression of the mitochondrial uncoupling protein gene from the aP2 gene promoter prevents genetic obesity. *J. Clin. Invest.* **1995**, *96*, 2914-2923. (d) Seale, P.; Conroe, H. M.; Estall, J.; Kajimura, S.; Frontini, A.; Ishibashi, J.; Cohen, P.; Cinti, S.; Spiegelman, B. M. Prdm16 determines the thermogenic program of subcutaneous white adipose tissue in mice. *J. Clin. Invest.* **2011**, *121*, 96-105.
4. (a) Virtanen, K. A.; Lidell, M. E.; Orava, J.; Heglind, M.; Westergren, R.; Niemi, T.; Taittonen, M.; Laine, J.; Savisto, N.-J.; Enerbäck, S.; Nuutila, P. Functional Brown Adipose Tissue in Healthy Adults. *New Engl. J. Med.* **2009**, *360*, 1518-1525. (b) Cypess, A. M.; Lehman, S.; Williams, G.; Tal, I.; Rodman, D.; Goldfine, A. B.; Kuo, F. C.; Palmer, E. L.; Tseng, Y.-H.; Doria, A.; Kolodny, G. M.; Kahn, C. R. Identification and Importance of Brown Adipose Tissue in Adult Humans. *New Engl. J. Med.* **2009**, *360*, 1509-1517.
5. Bostrom, P.; Wu, J.; Jedrychowski, M. P.; Korde, A.; Ye, L.; Lo, J. C.; Rasbach, K. A.; Bostrom, E. A.; Choi, J. H.; Long, J. Z.; Kajimura, S.; Zingaretti, M. C.; Vind, B. F.; Tu, H.; Cinti, S.; Hojlund, K.; Gygi, S. P.; Spiegelman, B. M. A PGC1-alpha-dependent myokine that drives brown-fat-like development of white fat and thermogenesis. *Nature* **2012**, *481*, 463-468.

6. Fisher, F. M.; Kleiner, S.; Douris, N.; Fox, E. C.; Mepani, R. J.; Verdeguer, F.; Wu, J.; Kharitononkov, A.; Flier, J. S.; Maratos-Flier, E.; Spiegelman, B. M. FGF21 regulates PGC-1 $\alpha$  and browning of white adipose tissues in adaptive thermogenesis. *Genes Dev.* **2012**, *26*, 271-281.
7. Peschechera, A.; Eckel, J. "Browning" of adipose tissue- regulation and therapeutic perspectives. *Arch. Physiol. Biochem.* **2013**, *119*, 151-160.
8. Harms, M.; Seale, P. Brown and beige fat: development, function and therapeutic potential. *Nat. Med.* **2013**, *19*, 1252-1263.
9. Dixen, K.; Basse, A. L.; Murholm, M.; Isidor, M. S.; Hansen, L. H.; Petersen, M. C.; Madsen, L.; Petrovic, N.; Nedergaard, J.; Quistorff, B.; Hansen, J. B. ERR $\gamma$  enhances UCP1 expression and fatty acid oxidation in brown adipocytes. *Obesity* **2013**, *21*, 516-24.
10. Mangelsdorf, D. J.; Thummel, C.; Beato, M.; Herrlich, P.; Schütz, G.; Umesono, K.; Blumberg, B.; Kastner, P.; Mark, M.; Chambon, P.; Evans, R. M. The Nuclear Receptor Superfamily: The Second Decade. *Cell* **1995**, *83*, 835-839.
11. (a) Hong, H.; Yang, L.; Stallcup, M. R. Hormone-independent Transcriptional Activation and Coactivator Binding by Novel Orphan Nuclear Receptor ERR3. *J. Biol. Chem.* **1999**, *274*, 22618-22626. (b) Heard, D. J.; Norby, P. L.; Holloway, J.; Vissing, H. Human ERR $\gamma$ , a Third Member of the Estrogen Receptor-Related Receptor (ERR) Subfamily of Orphan Nuclear Receptors: Tissue-Specific Isoforms Are Expressed during Development and in the Adult. *Mol. Endocrinol.* **2000**, *14*, 382-392. (c) Giguere, V. Transcriptional Control of Energy Homeostasis by the Estrogen-related Receptors. *Endocr. Rev.* **2008**, *29*, 677-696.
12. Wang, L.; Zuercher, W. J.; Consler, T. G.; Lambert, M. H.; Miller, A. B.; Orband-Miller, L. A.; McKee, D. D.; Willson, T. M.; Nolte, R. T. X-ray Crystal Structures of the Estrogen-related Receptor- Ligand Binding Domain in Three Functional States Reveal the Molecular Basis of Small Molecule Regulation. *J. Biol. Chem.* **2006**, *281*, 37773-37781.

13. (a) Zuercher, W. J.; Gaillard, S.; Orband-Miller, L. A.; Chao, E. Y. H.; Shearer, B. G.; Jones, D. G.; Miller, A. B.; Collins, J. L.; McDonnell, D. P.; Willson, T. M. Identification and Structure-Activity Relationship of Phenolic Acyl Hydrazones as Selective Agonists for the Estrogen-Related Orphan Nuclear Receptors ERR $\beta$  and ERR $\gamma$ . *J. Med. Chem.* **2005**, *48*, 3107-3109. (b) Kim, Y.; Koh, M.; Kim, D.-K.; Choi, H.-S.; Park, S. B. Efficient Discovery of Selective Small Molecule Agonists of Estrogen-Related Receptor  $\gamma$  using Combinatorial Approach. *J. Comb. Chem.* **2009**, *11*, 928-937.
14. Tron, G. C.; Pirali, T.; Billington, R. A.; Canonico, P. L.; Sorba, G.; Genazzani, A. A. Click chemistry reactions in medicinal chemistry: Applications of the 1,3-dipolar cycloaddition between azides and alkynes. *Med. Res. Rev.* **2008**, *28*, 278-308.
15. Xu, S.; Zhuang, X.; Pan, X.; Zhang, Z.; Duan, L.; Liu, Y.; Zhang, L.; Ren, X.; Ding, K. 1-Phenyl-4-benzoyl-1H-1,2,3-triazoles as Orally Bioavailable Transcriptional Function Suppressors of Estrogen-Related Receptor  $\alpha$ . *J. Med. Chem.* **2013**, *56*, 4631-4640.
16. Sanyal, S.; Kim, J.-Y.; Kim, H.-J.; Takeda, J.; Lee, Y.-K.; Moore, D. D.; Choi, H.-S. Differential Regulation of the Orphan Nuclear Receptor Small Heterodimer Partner (SHP) Gene Promoter by Orphan Nuclear Receptor ERR Isoforms. *J. Biol. Chem.* **2002**, *277*, 1739-1748.
17. Liu, D.; Zhang, Z.; Teng, C. T. Estrogen-related receptor- $\gamma$  and peroxisome proliferator-activated receptor- $\gamma$  coactivator-1 $\alpha$  regulate estrogen-related receptor- $\alpha$  gene expression via a conserved multi-hormone response element. *J. Mol. Endocrinol.* **2005**, *34*, 473-487.
18. (a) Dufour, C.; Wilson, B.; Huss, J.; Kelly, D.; Alaynick, W.; Downes, M.; Evans, R.; Blanchette, M.; Giguère, V. Genome-wide Orchestration of Cardiac Functions by the Orphan Nuclear Receptors ERR $\alpha$  and  $\gamma$ . *Cell Metab.* **2007**, *5*, 345-56. (b) Poidatz, D.; Dos Santos, E.; Brulé, A.; De Mazancourt, P.; Dieudonné, M. N. Estrogen-related receptor  $\gamma$  modulates energy metabolism target genes in human trophoblast. *Placenta* **2012**, *33*, 688-695.

19. Rangwala, S. M.; Wang, X.; Calvo, J. A.; Lindsley, L.; Zhang, Y.; Deyneko, G.; Beaulieu, V.; Gao, J.; Turner, G.; Markovits, J. Estrogen-related Receptor  $\gamma$  Is a Key Regulator of Muscle Mitochondrial Activity and Oxidative Capacity. *J. Biol. Chem.* **2010**, *285*, 22619-22629.
20. Seale, P.; Bjork, B.; Yang, W.; Kajimura, S.; Chin, S.; Kuang, S.; Scime, A.; Devarakonda, S.; Conroe, H. M.; Erdjument-Bromage, H.; Tempst, P.; Rudnicki, M. A.; Beier, D. R.; Spiegelman, B. M. PRDM16 controls a brown fat/skeletal muscle switch. *Nature* **2008**, *454*, 961-967.
21. (a) Alaynick, W. A.; Kondo, R. P.; Xie, W.; He, W.; Dufour, C. R.; Downes, M.; Jonker, J. W.; Giles, W.; Naviaux, R. K.; Giguere, V.; Evans, R. M. ERR $\gamma$  Directs and Maintains the Transition to Oxidative Metabolism in the Postnatal Heart. *Cell Metab.* **2007**, *6*, 13-24. (b) Ventura-Clapier, R.; Garnier, A.; Veksler, V. Transcriptional control of mitochondrial biogenesis: the central role of PGC-1 $\alpha$ . *Cardiovasc. Res.* **2008**, *79*, 208-217.
22. Saeed, H.; Taipaleenmäki, H.; Aldahmash, A.; Abdallah, B.; Kassem, M. Mouse Embryonic Fibroblasts (MEF) Exhibit a Similar but not Identical Phenotype to Bone Marrow Stromal Stem Cells (BMSC). *Stem Cell Rev. & Rep.* **2012**, *8*, 318-328.
23. (a) Matsumoto, T.; Kano, K.; Kondo, D.; Fukuda, N.; Iribe, Y.; Tanaka, N.; Matsubara, Y.; Sakuma, T.; Satomi, A.; Otaki, M.; Ryu, J.; Mugishima, H. Mature adipocyte-derived dedifferentiated fat cells exhibit multilineage potential. *J. Cell. Physiol.* **2008**, *215*, 210-222. (b) Fasshauer, M.; Klein, J.; Kriauciunas, K. M.; Ueki, K.; Benito, M.; Kahn, C. R. Essential Role of Insulin Receptor Substrate 1 in Differentiation of Brown Adipocytes. *Mol. Cell. Biol.* **2001**, *21*, 319-329.

## Graphic Content



ACCEPTED MANUSCRIPT